EDISON

Electromagnetic Design of
flexIble SensOrs

FNP Team-Tech

# Spurious modes in local model order reduction

Martyna Czarniewska
April 30, 2018

European Funds Smart Growth

FNP Foundation for Polish Science

European Union
European Regional Development Fund

This work was supported by project EDISOn - Electromagnetic Design of FlexIbleSensOrs, The „EDISOn" project is carried out within the TEAM-TECH programme of the Foundation for Polish Science co-financed by the European Union under the European Regional Development Fund.

| Revision | Date | Author(s) | Description |
|---|---|---|---|
| 1.0 | 13.03.2018 | M. Czarniewska | created |
| 2.0 | 20.03.2018 | M. Czarniewska | added new results |
| 3.0 | 28.03.2018 | M. Czarniewska | results of dual-mode filter analysis added |

# 1 Introduction

- We consider the 5-th order waveguide filter divided into 7 subdomains - the analyzed geometry as well as the segmentation are shown in Fig. 1.
- 11 geometry parameters are defined: 2, 2, 3, 2, 2 in $\Omega_2$, $\Omega_3$, $\Omega_4$, $\Omega_5$, $\Omega_6$, respectively. The mesh is deformed locally within subdomains, while mesh deformation technique based on triharmonic radial basis functions was used. The initial values of all parameters and the range of allowable parameter variations are shown in Table 2.

| domain | parameter | Initial (mm) | Min (mm) | Max (mm) |
|---|---|---|---|---|
| $\Omega_2$ | $d_1$ | 2.000 | 1.000 | 3.000 |
| | $R_1$ | 12.188 | 10.188 | 14.188 |
| $\Omega_3$ | $h_1$ | 5.456 | 2.450 | 8.450 |
| | $w_1$ | 2.430 | 1.430 | 5.430 |
| $\Omega_4$ | $W$ | 27.805 | 26.805 | 28.805 |
| | $L_1$ | 12.194 | 8.194 | 16.194 |
| | $L_2$ | 16.743 | 12.743 | 20.743 |
| $\Omega_5$ | $h_2$ | 5.949 | 2.949 | 8.949 |
| | $w_2$ | 2.430 | 1.430 | 5.430 |
| $\Omega_6$ | $d_2$ | 2.000 | 1.000 | 3.000 |
| | $R_2$ | 12.264 | 10.264 | 14.264 |

Table 2: Initial values of geometry parameters and variation range

- The frequency bandwidth of interest is 9-11 GHz.
- Figures 2 and 3 show the Z and S parameters of the filter.
- There are 5 resonant frequencies of the filter in the frequency band of interest (in GHz):

| filter eigenresonances (GHz) |
|---|
| 9.7658 |
| 9.8120 |
| 9.9450 |
| 10.0758 |
| 10.1578 |

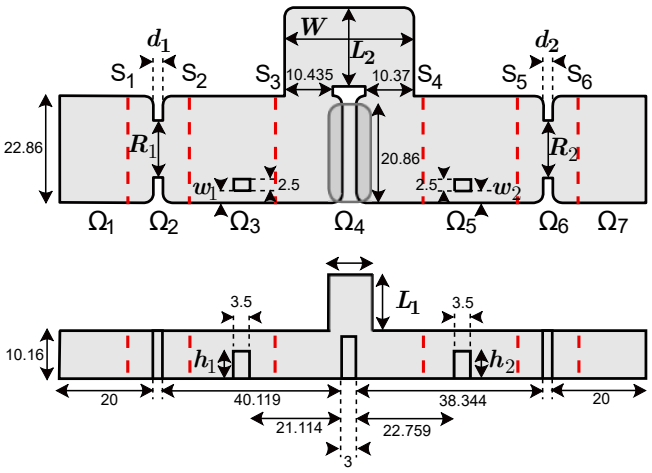


Figure 1: Geometry of the 5th order waveguide filter.

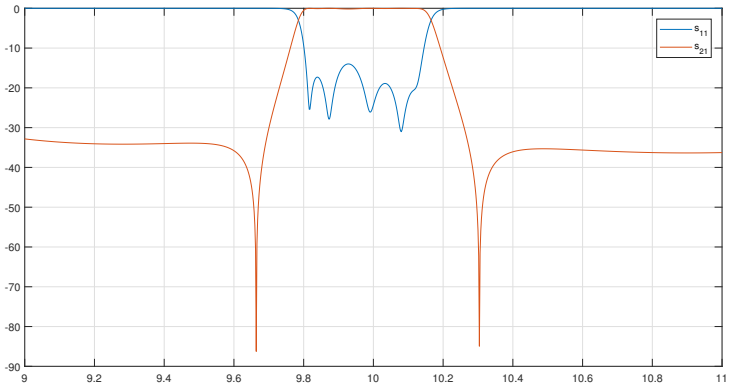


Figure 2: Scattering parameters.

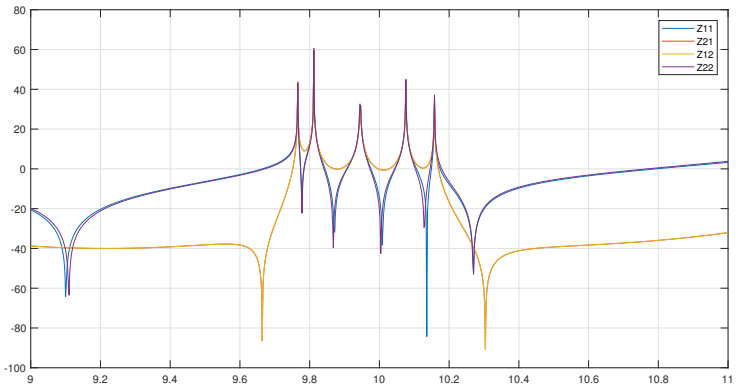


Figure 3: Impedance.

## 2 Non-physical solutions

The problem of non-physical solutions occurs when geometry model-order reduction is applied. In order to show the behaviour of the spurious eigenmodes and present schemes of identifying them, we analyse the waveguide filter shown in Fig. 1 and apply geometry model order reduction in one subdomain $\Omega_5$. The rest of the computational domain was subject to standard local model order reduction with

| parameter | $\mathcal{G}_1$ | $\mathcal{G}_2$ | $\mathcal{G}_3$ | $\mathcal{G}_4$ |
|---|---|---|---|---|
| $h_2$ [mm] | -2.3 | -2.39 | -1.64 | -2.23 |
| $w_2$ [mm] | 1.39 | -1.28 | -2.45 | 1.1 |

Table 3: Change in geometry parameters in $\Omega_5$, $\mathcal{G}_1$, $\mathcal{G}_2$, $\mathcal{G}_3$, $\mathcal{G}_4$ - geometry instances used to generate projection basis

frequency as parameter. Parametrized projection basis $\mathbf{Q}^{\mathcal{P}}$ contained vectors of **4 different bases** associated with 4 different geometries of subdomain $\Omega_5$.

After applying the parametric model order reduction in $\Omega_5$ with basis $\mathbf{Q}^{\mathcal{P}}$ and solving the problem we get the filter response shown in the Figures 4 and 5. Spurious resonances can be seen in the scattering parameters plot as well as in the impedance plot.

Solution of the eigenproblem brings about the 11 eigenresonances in band of analysis (see Table 4): 5 true and 6 spurious.

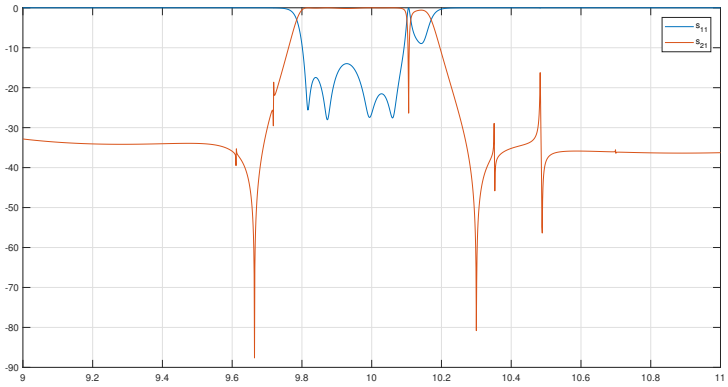


Figure 4: Scattering parameters with spurious modes.

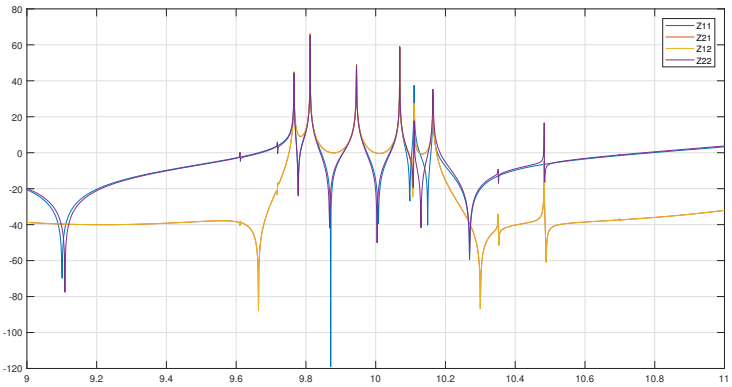


Figure 5: Impedance with spurious modes.

| eigenresonances (global) [GHz] |
|---|
| 9.6113 |
| 9.7185 |
| **9.7659** |
| **9.8120** |
| **9.9449** |
| **10.0690** |
| 10.1102 |
| **10.1643** |
| 10.3515 |
| 10.4829 |
| 10.6994 |

Table 4: Eigenresonances of the structure - spurious (normal font) and true (bold font)

## 2.1 Analysis of spurious modes in macromodel

Reduced FE matrices consist of small and dense blocks (macromodels) and have sparsity pattern shown in Fig. 6. The behaviour of the electromagnetic field in subdomain $\Omega_5$ is determined by the local system of equations:

$$(\mathbf{\Gamma}_{\Omega_5} - k^2\mathbf{C}_{\Omega_5}) \cdot \mathbf{E}_{\Omega_5} = -(\mathbf{G}_{\delta\Omega_5} - k^2\mathbf{T}_{\delta\Omega_5}) \cdot \mathbf{E}_{\delta\Omega_5} \tag{1}$$

where $\mathbf{G}_{\delta\Omega_5}$ and $\mathbf{T}_{\delta\Omega_5}$ are blocks describing the coupling between subregion $\Omega_5$ and interfaces $S_4$, $S_5$, $\mathbf{E}_{\Omega_5}$ contains coefficients associated with FE basis functions in $\Omega_5$ and $\mathbf{E}_{\delta\Omega_5}$ contains coefficients associated with FE basis functions in the boundary $\delta\Omega_5 = \{S_4, S_5\}$.

Model order reduction results in the reduced system of equations:

$$(\widetilde{\mathbf{\Gamma}}_{\Omega_5} - k^2\widetilde{\mathbf{C}}_{\Omega_5}) \cdot \widetilde{\mathbf{E}}_{\Omega_5} = -(\widetilde{\mathbf{G}}_{\delta\Omega_5} - k^2\widetilde{\mathbf{T}}_{\delta\Omega_5}) \cdot \mathbf{E}_{\delta\Omega_5} \tag{2}$$

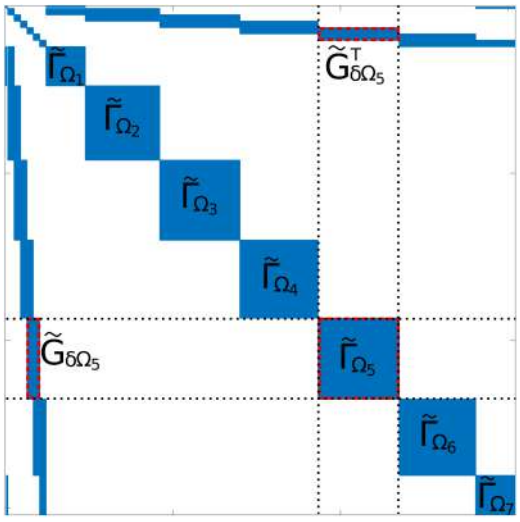


Figure 6: Sparsity pattern of the reduced matrix $\widetilde{\mathbf{\Gamma}}$.

Solving the reduced generalized eigenproblem

$$(\widetilde{\mathbf{\Gamma}}_{\Omega_5} - k_i^2\widetilde{\mathbf{C}}_{\Omega_5}) \cdot \widetilde{\mathbf{v}}_i = 0 \tag{3}$$

results in the eigenresonanses $f_i = c \cdot k_i/(2\pi)$ of the macromodel and the corresponding eigenvectors $\widetilde{\mathbf{v}}_i$.

In this example, we get 6 eigenresonanses of macromodel $\Omega_5$ (all of them are spurious). Note, that these values are similar to spurious frequencies of the global model in Table 4.

| eigenresonances in $\Omega_5$ [GHz] |
|---|
| 9.6120 |
| 9.7206 |
| 10.1111 |
| 10.3513 |
| 10.4797 |
| 10.6993 |

Table 5: Eigenresonances of macromodel in $\Omega_5$

If we remove all these spurious eigenresonances from the projection basis (i.e. via deflation) we obtain 5 true resonances in band: 9.7658 GHz, 9.8120 GHz, 9.9453 GHz, 10.0767 GHz, 10.1590 GHz and smooth filter response (see Figures 7 and 8). The comparison of the local estimated error of the macromodel [1] containing spurious modes and the macromodel after deflation (after removing spurious eigenmodes from the projection basis) is shown in Fig. 9.

The crucial issue is to automatically identify, which eigenresonance is spurious. In the next subsections different schemes of identifying spurious modes are described.

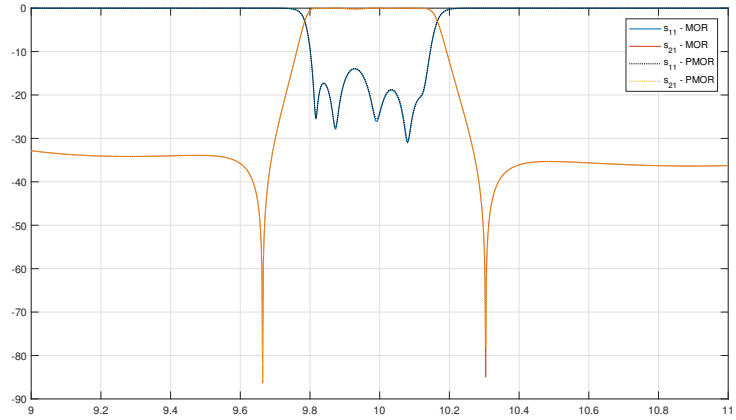


Figure 7: Scattering parameters after deleting spurious modes.

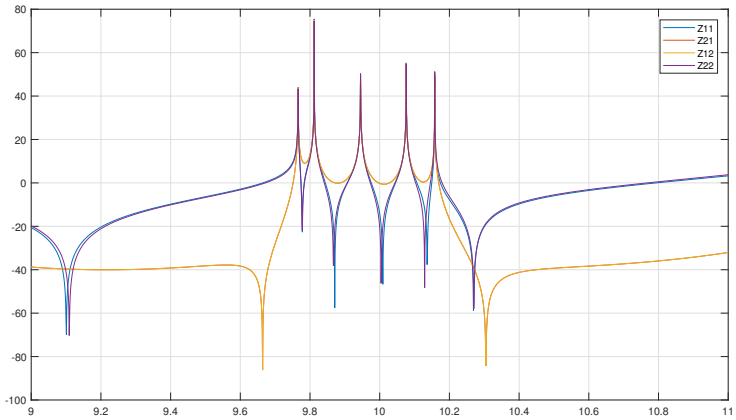


Figure 8: Impedance after deleting spurious modes.

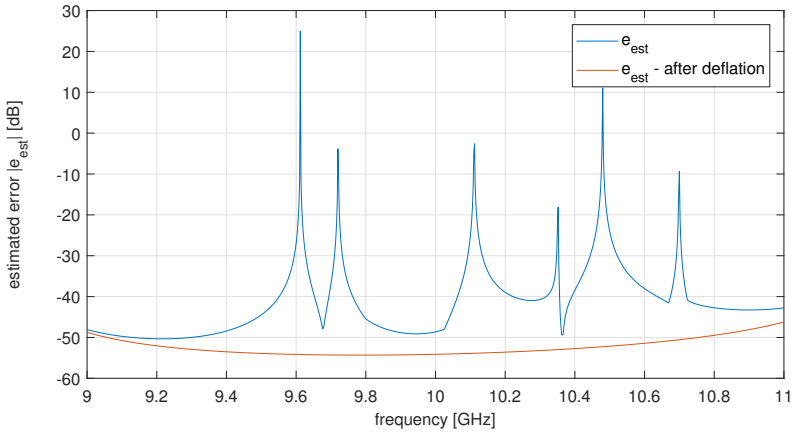


Figure 9: Local error estimator before and after deflation.

## 2.2 Residual errors of eigenvalue problem

If the quality of the projection basis is good, eigenvectors of the reduced-order model are good approximation of the eigenvectors of the original model and they should give value equal to zero (or close to zero) of the residual error (4):

$$R = \| \left(\mathbf{\Gamma}_{\Omega_5} - k_i^2 \mathbf{C}_{\Omega_5}\right) \cdot \mathbf{Q}\widetilde{\mathbf{v}}_i \|_2 \tag{4}$$

On the other hand, spurious modes are not the solution of the original eigenproblem so they should give high value of the residue. Residual errors for six eigenvectors are shown in Table 6 - all values are about 0.1.

| eigenfrequency [GHz] | Residue |
|---|---|
| 9.6120 | 0.0883 |
| 9.7206 | 0.0895 |
| 10.1111 | 0.1206 |
| 10.3513 | 0.0994 |
| 10.4797 | 0.1030 |
| 10.6993 | 0.0997 |

Table 6: Values of residual errors of local eigenproblem in $\Omega_5$

## 2.3 Perturbation analysis

We use Bauer-Fike theorem to compute the bound of the shift of eigenvalues when FE matrices undergo a defined perturbation. Firstly, FE matrices are diagonalized by means of the procedure described in 2.3.1. The sparsity pattern of the FE matrices after diagonalization procedure is shown in Fig. 10.

We define:

- the pair ($\widetilde{\mathbf{\Gamma}}_0$, $\widetilde{\mathbf{C}}_0$), where $\widetilde{\mathbf{\Gamma}}_0$, $\widetilde{\mathbf{C}}_0$ are strictly diagonal, with eigenvalues and eigenvectors ($\lambda_{0_i}$, $\mathbf{x}_{0_i}$);
- perturbation matrices are coupling matrices (see Fig. 11);
- matrices containing perturbation ($\widetilde{\mathbf{\Gamma}}$, $\widetilde{\mathbf{C}}$) with corresponding $\lambda_i$.

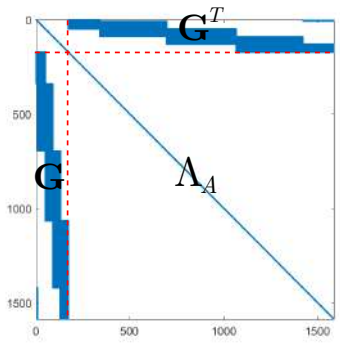


Figure 10: Sparsity pattern of the diagonalized FE matrices.

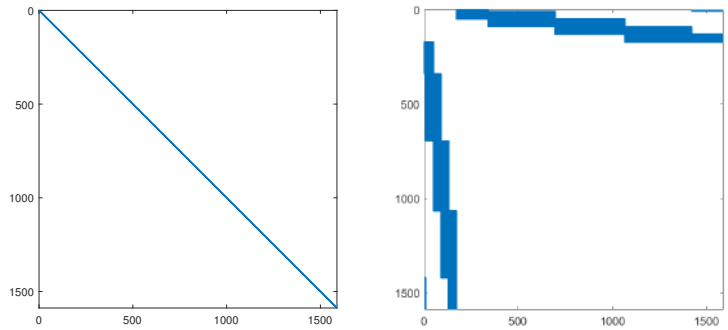


Figure 11: (a) Sparsity pattern of matrices $\widetilde{\mathbf{\Gamma}}_0$, $\widetilde{\mathbf{C}}_0$. (b) Sparsity pattern of coupling matrices (perturbation matrices).

Error bound $\Delta\lambda_{i(est)}$ for $i$-th eigenvalue in Bauer-Fike theorem [2] is defined

$$|\widetilde{\lambda}_i - \lambda_i| \leq \Delta\lambda_{i(est)} = \| \widetilde{\mathbf{C}}^{-1} \| \cdot \| \mathbf{r} \|, \tag{5}$$

where $\| \mathbf{r} \|$ is a norm of the residual vector

$$\| \mathbf{r} \| = (\widetilde{\mathbf{\Gamma}} - \lambda_{0_i} \widetilde{\mathbf{C}}) \cdot \mathbf{x}_{0_i}, \tag{6}$$

$\lambda_{0_i}$ is the eigenvalue of the reduced local eigenproblem with diagonal matrices ($\widetilde{\mathbf{\Gamma}}_0$, $\widetilde{\mathbf{C}}_0$), $\lambda_i$ is the eigenvalue of the local eigenproblem with perturbation ($\widetilde{\mathbf{\Gamma}}$, $\widetilde{\mathbf{C}}$) and $\mathbf{x}_{0_i}$ is the eigenvector associated with $i$-th eigenvalue $\lambda_{0_i}$.

In our case, matrices ($\widetilde{\mathbf{\Gamma}}_0$, $\widetilde{\mathbf{C}}_0$) are strictly diagonal (they do not contain coupling matrices) while ($\widetilde{\mathbf{\Gamma}}$, $\widetilde{\mathbf{C}}$) are matrices with coupling blocks. Small values of $\Delta\lambda_{i(est)}$ are associated with spurious resonances since they do not shift significantly (they are not excited). Since $\| \widetilde{\mathbf{C}}^{-1} \|$ is the same for all eigenvalues, observation of $\| \mathbf{r} \|$ is enough to determine if resonance is true or spurious.

### 2.3.1 Converting the FE system into symmetric eigenproblem

Symmetrization procedure of the local non-symmetric eigenvalue problem defined in equation (3) is described below. Initially, we compute $\widetilde{\mathbf{C}}_{\Omega_5}^{\frac{1}{2}}$ via the eigendecomposition of matrix $\widetilde{\mathbf{\Gamma}}_{\Omega_5}$:

$$\widetilde{\mathbf{C}}_{\Omega_5} = \mathbf{V}\mathbf{\Lambda}\mathbf{V}^T, \tag{7}$$

$$\widetilde{\mathbf{C}}_{\Omega_5}^{\frac{1}{2}} = \mathbf{V}\mathbf{\Lambda}^{\frac{1}{2}}\mathbf{V}^T. \tag{8}$$

Similarly, $\widetilde{\mathbf{C}}_{\Omega_5}^{-\frac{1}{2}}$ is:

$$\widetilde{\mathbf{C}}_{\Omega_5}^{-\frac{1}{2}} = \mathbf{V}\mathbf{\Lambda}^{-\frac{1}{2}}\mathbf{V}^T. \tag{9}$$

Then, we multiply equation (2) by $\widetilde{\mathbf{C}}_{\Omega_5}^{-\frac{1}{2}}$ which results in the following form:

$$(\widetilde{\mathbf{C}}_{\Omega_5}^{-\frac{1}{2}}\widetilde{\mathbf{\Gamma}}_{\Omega_5}\widetilde{\mathbf{C}}_{\Omega_5}^{-\frac{1}{2}}\widetilde{\mathbf{C}}_{\Omega_5}^{\frac{1}{2}} - k^2\mathbf{I}\widetilde{\mathbf{C}}_{\Omega_5}^{\frac{1}{2}}) \cdot \widetilde{\mathbf{E}}_{\Omega_5} = -(\widetilde{\mathbf{C}}_{\Omega_5}^{-\frac{1}{2}}\widetilde{\mathbf{G}}_{\delta\Omega_5} - k^2\widetilde{\mathbf{C}}_{\Omega_5}^{-\frac{1}{2}}\widetilde{\mathbf{T}}_{\delta\Omega_5}) \cdot \mathbf{E}_{\delta\Omega_5}, \tag{10}$$

$$(\widetilde{\mathbf{C}}_{\Omega_5}^{-\frac{1}{2}}\widetilde{\mathbf{\Gamma}}_{\Omega_5}\widetilde{\mathbf{C}}_{\Omega_5}^{-\frac{1}{2}} - k^2\mathbf{I}) \cdot \widetilde{\mathbf{C}}_{\Omega_5}^{\frac{1}{2}}\widetilde{\mathbf{E}}_{\Omega_5} = -(\widetilde{\mathbf{C}}_{\Omega_5}^{-\frac{1}{2}}\widetilde{\mathbf{G}}_{\delta\Omega_5} - k^2\widetilde{\mathbf{C}}_{\Omega_5}^{-\frac{1}{2}}\widetilde{\mathbf{T}}_{\delta\Omega_5}) \cdot \mathbf{E}_{\delta\Omega_5}, \tag{11}$$

where $\mathbf{I}$ is identity matrix. We rewrite the equation (11) in a form:

$$(\mathbf{A} - k^2\mathbf{I}) \cdot \widetilde{\mathbf{C}}_{\Omega_5}^{\frac{1}{2}}\widetilde{\mathbf{E}}_{\Omega_5} = -\mathbf{D}(k) \cdot \mathbf{E}_{\delta\Omega_5}, \tag{12}$$

where $\mathbf{A}$ is symmetric matrix

$$\mathbf{A} = \widetilde{\mathbf{C}}_{\Omega_5}^{-\frac{1}{2}}\widetilde{\mathbf{\Gamma}}_{\Omega_5}\widetilde{\mathbf{C}}_{\Omega_5}^{-\frac{1}{2}}$$

and $\mathbf{D}$ is the right-hand side of the symmetric problem (11)

$$\mathbf{D}(k) = \widetilde{\mathbf{C}}_{\Omega_5}^{-\frac{1}{2}}\widetilde{\mathbf{G}}_{\delta\Omega_5} - k^2\widetilde{\mathbf{C}}_{\Omega_5}^{-\frac{1}{2}}\widetilde{\mathbf{T}}_{\delta\Omega_5}. \tag{13}$$

Now, we compute eigenvalues $\lambda_i$ and eigenvectors $\mathbf{v}_i$ of the symmetric problem (14):

$$\begin{aligned}(\mathbf{A} - k^2\mathbf{I}) \cdot \mathbf{V}_S &= 0, \\ \mathbf{A} &= \widetilde{\mathbf{C}}_{\Omega_5}^{-\frac{1}{2}}\widetilde{\mathbf{\Gamma}}_{\Omega_5}\widetilde{\mathbf{C}}_{\Omega_5}^{-\frac{1}{2}}, \\ \mathbf{V}_S &= \widetilde{\mathbf{C}}_{\Omega_5}^{\frac{1}{2}}\widetilde{\mathbf{E}}_{\Omega_5}.\end{aligned} \tag{14}$$

We perform the eigendecomposition of the symmetric matrix $\mathbf{A} = \widetilde{\mathbf{C}}_{\Omega_5}^{-\frac{1}{2}}\widetilde{\mathbf{\Gamma}}_{\Omega_5}\widetilde{\mathbf{C}}_{\Omega_5}^{-\frac{1}{2}}$ and convert the equation (12):

$$(\mathbf{V}_A\mathbf{\Lambda}_A\mathbf{V}_A^T - k^2\mathbf{I}) \cdot \widetilde{\mathbf{C}}_{\Omega_5}^{\frac{1}{2}}\widetilde{\mathbf{E}}_{\Omega_5} = -\mathbf{D} \cdot \mathbf{E}_{\delta\Omega_5}, \tag{15}$$

$$\mathbf{V}_A(\mathbf{\Lambda}_A - k^2\mathbf{V}_A^T\mathbf{I}\mathbf{V}_A) \cdot \mathbf{V}_A^T\widetilde{\mathbf{C}}_{\Omega_5}^{\frac{1}{2}}\widetilde{\mathbf{E}}_{\Omega_5} = -\mathbf{D} \cdot \mathbf{E}_{\delta\Omega_5}, \tag{16}$$

$$(\mathbf{\Lambda}_A - k^2\mathbf{I}) \cdot \underbrace{\mathbf{V}_A^T\widetilde{\mathbf{C}}_{\Omega_5}^{\frac{1}{2}}\widetilde{\mathbf{E}}_{\Omega_5}}_{\hat{\mathbf{E}}_{\Omega_5}} = -\mathbf{V}_A^T\mathbf{D} \cdot \mathbf{E}_{\delta\Omega_5}, \tag{17}$$

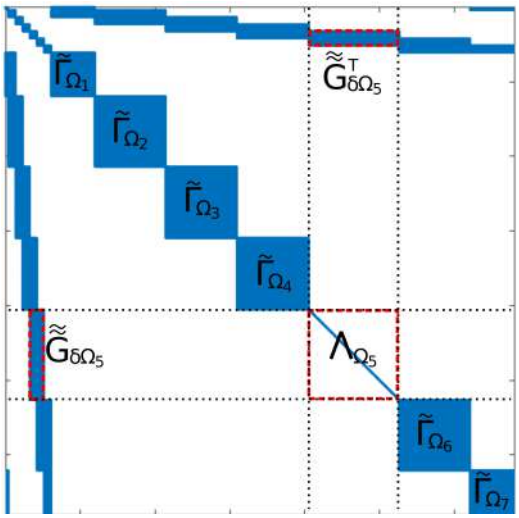


Figure 12: Sparsity pattern of the reduced matrix $\widetilde{\mathbf{\Gamma}}$ with diagonalized macromodel $\Omega_5$

# 3 Numerical results

## 3.1 Test 1: parametric model order reduction in 5 subdomains: $\Omega_2$, $\Omega_3$, $\Omega_4$, $\Omega_5$, $\Omega_6$

Applying geometry model order reduction in 5 subdomains of the waveguide filter shown in Fig. 1 resulted in 19 resonances in frequency band of analysis (5 true and 14 spurious) - see Table 7. Bases associated with 2, 3, 3, 3, 2 geometries were used in subdomains $\Omega_2$, $\Omega_3$, $\Omega_4$, $\Omega_5$, $\Omega_6$, respectively. Frequency response of the filter is shown in Fig. 13.

| eigenresonances (global) [GHz] |
|---|
| **9.7660** |
| **9.8123** |
| **9.9453** |
| **10.0760** |
| **10.1579** |
| 9.0405 |
| 9.1134 |
| 9.3488 |
| 9.6035 |
| 10.0845 |
| 10.6862 |
| 10.8953 |
| 9.3271 |
| 10.4640 |
| 9.5076 |
| 10.0020 |
| 10.6363 |
| 10.7804 |
| 9.7664 |

Table 7: Eigenresonances of the structure - spurious (normal font) and true (bold font)

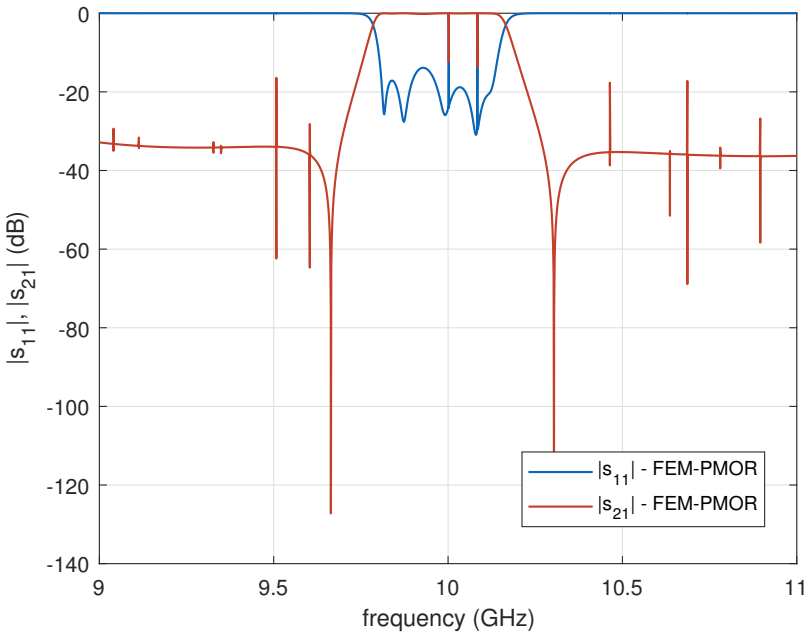


Figure 13: Filter response with spurious modes

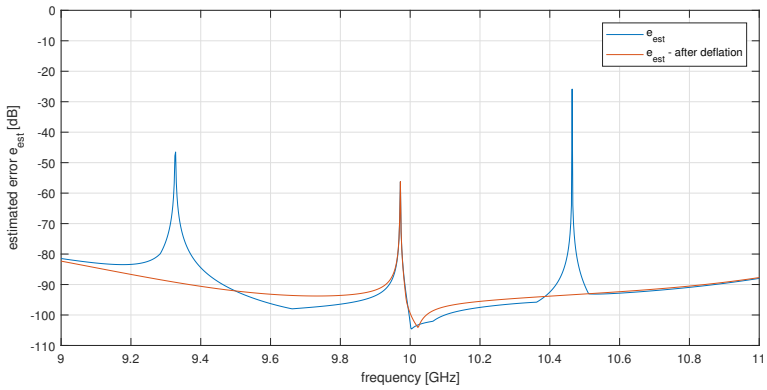


Figure 14: Local estimated error in subdomain $\Omega_4$ after removing two spurious modes from the ROM compared to estimated error before deflation

### 3.2 Analysis of spurious modes in macromodels

Table 3.2 shows true eigenfrequencies in band for each of 5 analysed macromodels as well as eigenfrequencies computed for the reduced order model obtained by means of geometry model order reduction. There is only one true resonanse in $\Omega_4$. Note, that spurious modes of macromodels are approximately the same as spurious modes of global model in Table 7.

| | $\Omega_2$ | $\Omega_3$ | $\Omega_4$ | $\Omega_5$ | $\Omega_6$ |
|---|---|---|---|---|---|
| true $f_{res}$ [GHz] | - | - | 9.9716 | - | - |
| true+spurious $f_{res}$ [GHz] (computed for parameterized macromodel) | 9.7663 | 9.5076<br>10.0020<br>10.6363<br>10.7804 | 9.3271<br>**9.9716**<br>10.4640 | 9.0405<br>9.1134<br>9.3488<br>9.6037<br>10.0844<br>10.6862<br>10.8952 | - |

Table 8: Eigenresonances of 5 local models - $\Omega_2$, $\Omega_3$, $\Omega_4$, $\Omega_5$, $\Omega_6$

In Table 9 residual errors for true and spurious resonances in subdomain $\Omega_4$ are compared. Since the projection basis is good enough and allows to approximate the true eigenvector of the original model accurately, associated residue is small (2.49e-05). Two spurious modes are not the solution of the original model, so corresponding residual errors are much higher. Figure 14 shows local estimated error in subdomain $\Omega_4$ after removing two spurious modes from the ROM compared to estimated error before deflation.

| eigenresonance [GHz] | residual error |
|---|---|
| 9.3271 | 0.0918 |
| **9.9716** | **2.49e-05** |
| 10.4640 | 0.1089 |

Table 9: Residual errors for eigenvectors in $\Omega_4$

Residues defined in (4) and (6) were computed for all eigenresonances in subdomains $\Omega_2$, $\Omega_3$, $\Omega_4$, $\Omega_5$ - see Figures 16 and 15.

Estimated local error in $\Omega_2$, $\Omega_3$, $\Omega_4$, $\Omega_5$ and $\Omega_6$ is shown in Fig. 17.

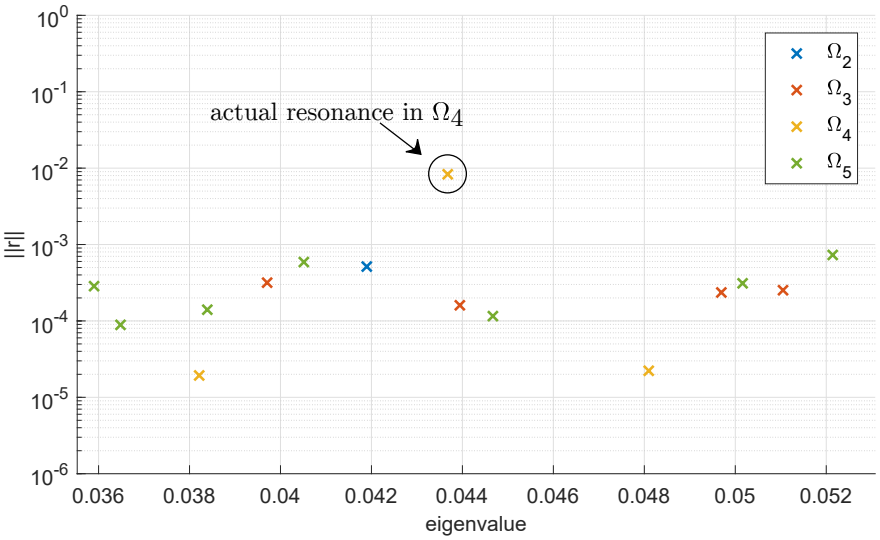


Figure 15: Residues for eigenvalues of the local ROMs (6).

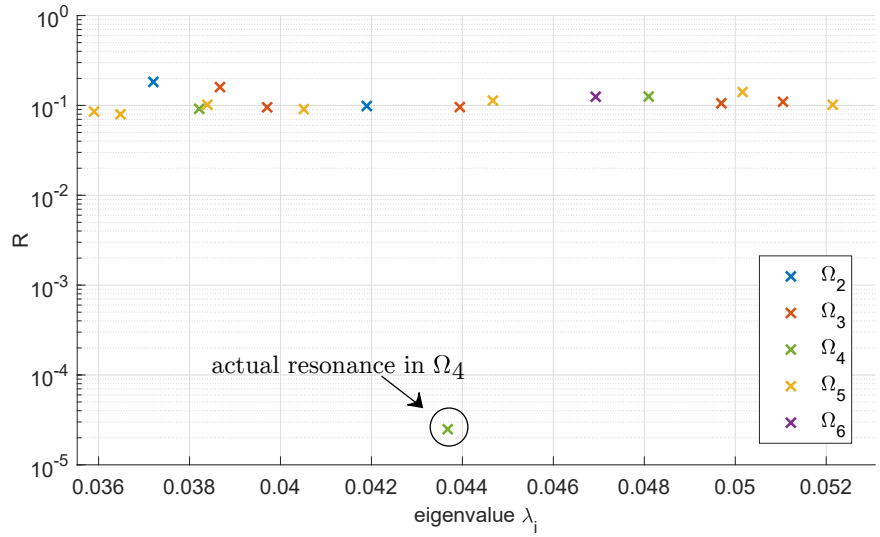


Figure 16: Residues for eigenvalues of the local ROMs (4).

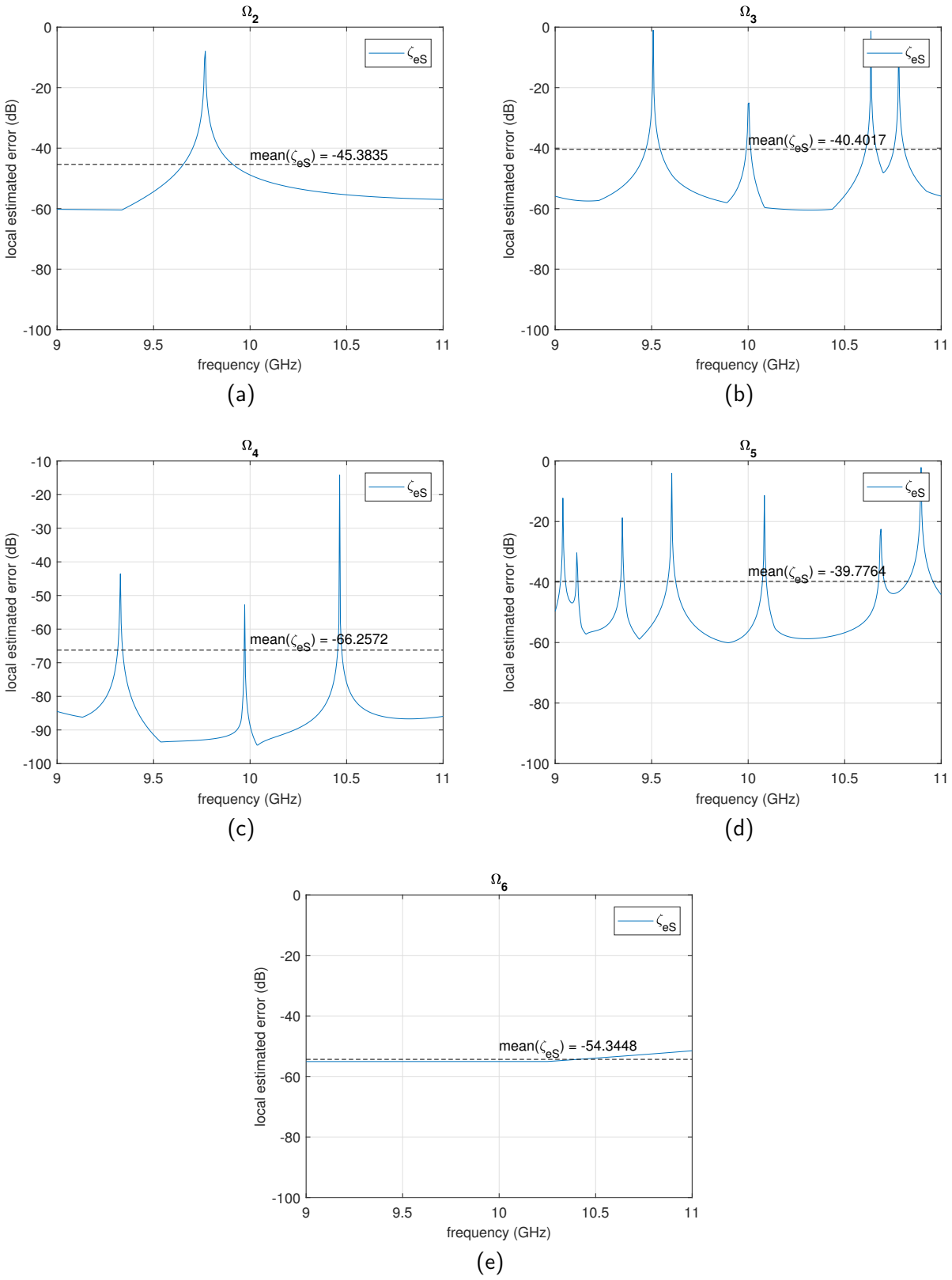


Figure 17: Local estimated error in 5 macromodels.

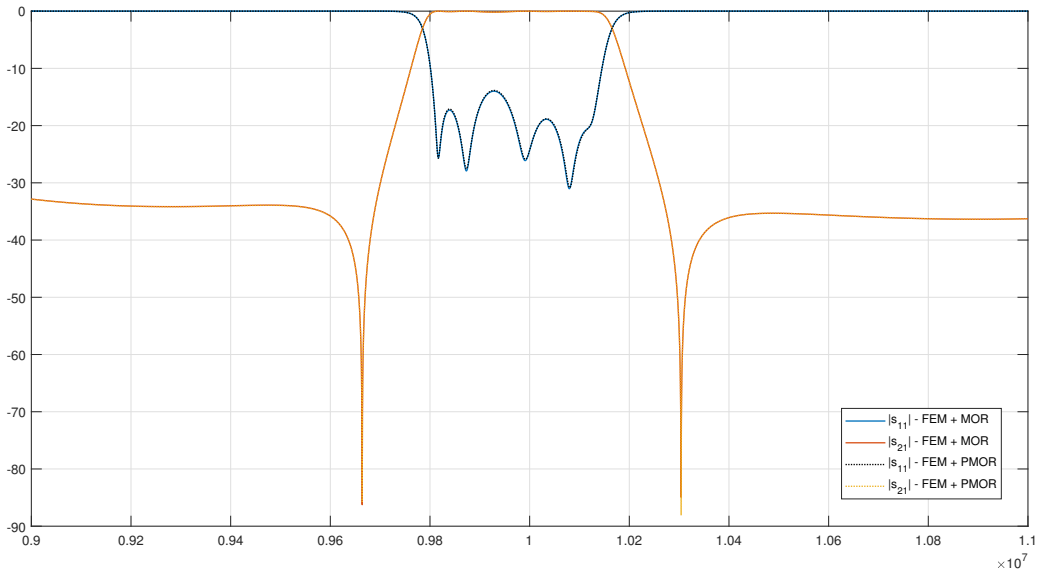


Figure 18: Filter response after deleting spurious modes

Eigenresonances in band after deleting spurious modes in macromodels (in GHz): 9.7660, 9.8123, 9.9453, 10.0761, 10.1579.

### 3.3 Test 2: Wideband analysis with GMOR in $\Omega_4$

In order to obtain results with numerous true resonances in band, wideband analysis was performed. Frequency band of interest was from 7 to 11 GHz. Geometry model order reduction was applied in $\Omega_4$. Parametrized projection basis $\mathbf{Q}^{\mathcal{P}}$ contained vectors of **3 different bases** associated with 3 different geometries of subdomain $\Omega_4$.

Solution of the local eigenvalue problem resulted in 18 resonances, while 3 of them were true. Associated residual errors defined in eq. (4) and (6) are shown in Fig.

Fig. 22 shows local estimated error.

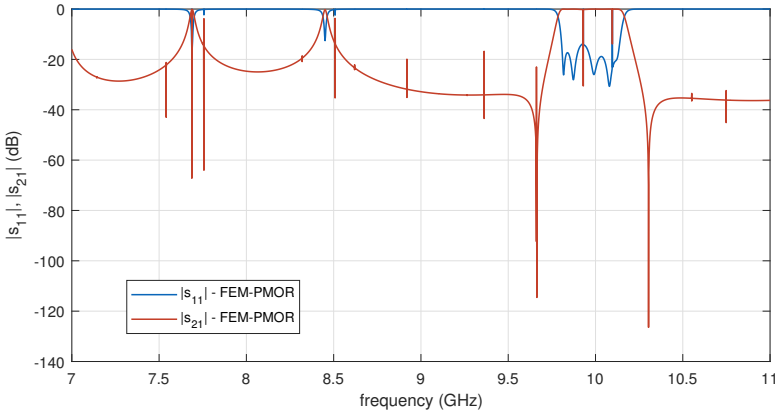


Figure 19: Scattering parameters in frequency band 7-11 GHz.

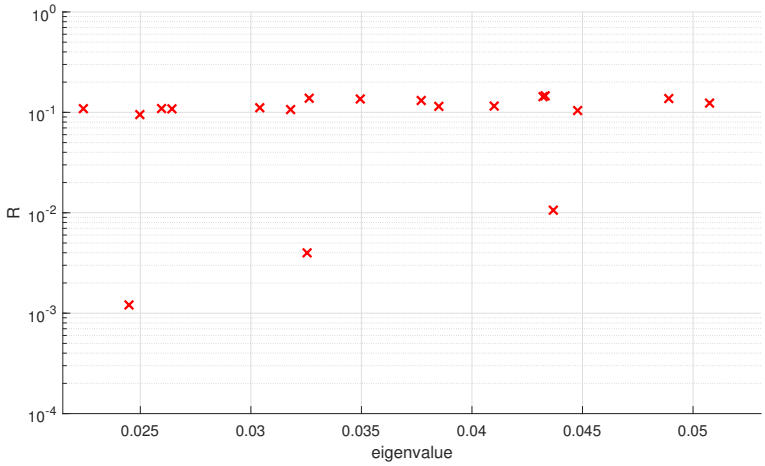


Figure 20: Residues for eigenvalues of the local ROM (4).

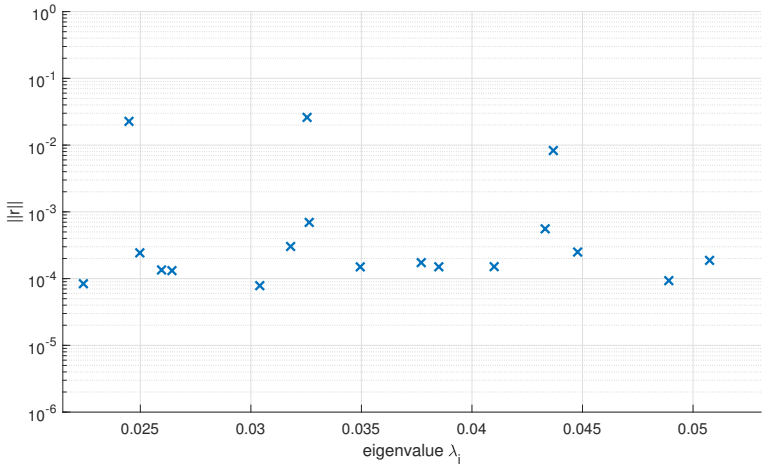


Figure 21: Residues for eigenvalues of the local ROM (6).

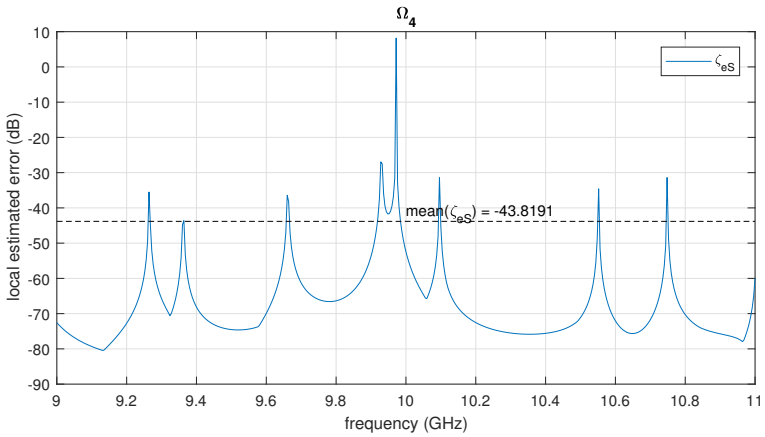


Figure 22: Local estimated error.

Scattering parameters after deflation are presented in Fig. 23.

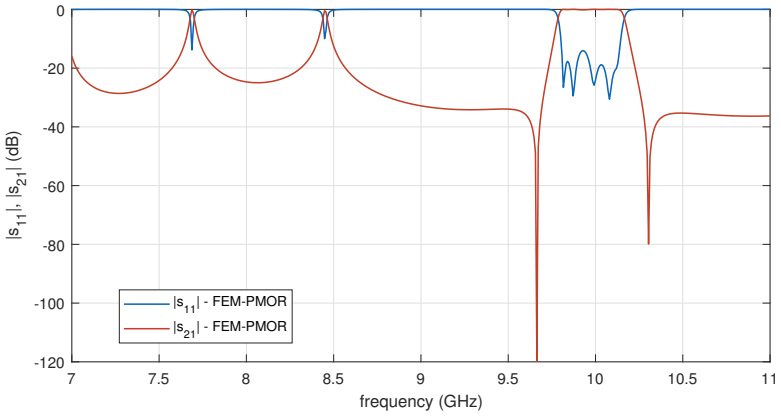


Figure 23: Scattering parameters for the ROM after deflation.

### 3.4 Dual-mode filter

- The analysed structure segmented into 5 subdoamains is shown in the Fig. 24.
- Two subdomains – $\Omega_2$ and $\Omega_4$ – are subject to geometry modification – lengths of the tuning screws are modified.
- Frequency band of interest – 11.4 - 12.4 GHz.
- 4 resonant frequencies of the filter in the frequency band of interest (in GHz):

| filter eigenresonances (GHz) |
|---|
| 11.7546 |
| 11.7987 |
| 11.8801 |
| 11.8828 |

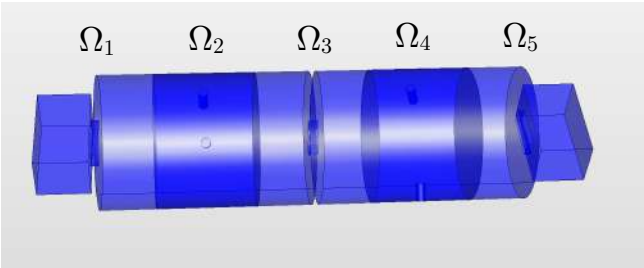


Figure 24: Dual-mode filter segmented into 5 subdomains.

Firstly, PMOR was applied only in $\Omega_4$. Parametrized projection basis $\mathbf{Q}^{\mathcal{P}}$ consisting of three local bases: $\mathbf{Q}^{\mathcal{P}} = \text{SVD}([[\mathbf{Q}_1, \mathbf{Q}_2, \mathbf{Q}_3]])$ was used, while $\{\mathbf{Q}_1, \mathbf{Q}_2, \mathbf{Q}_3\}$ are bases computed for three different geometries of $\Omega_4$. This resulted in spurious resonances of the ROM what might be observed in the frequency response depicted in Fig. 25.

The basis $\mathbf{Q}^{\mathcal{P}}$ consisted of 1701 vectors, basis compression reduced the number of vectors to 355.

Local ROM contains only 2 actual eigenvalues in band of interest. Projection using parametrized basis $\mathbf{Q}^{\mathcal{P}}$ produced 6 additional spurious eigenvalues - see Fig. 26. This results in 6 spurious eigenvalues in global ROM (Fig. 27).

In order to automatically identify and deflate spurious modes from the local ROM, local estimated error needs to be evaluated. Local estimated error of the ROM in $\Omega_4$ is shown in Fig. 28. Mean value of the local error is -60 dB, which means that the macromodel is accurate enough.

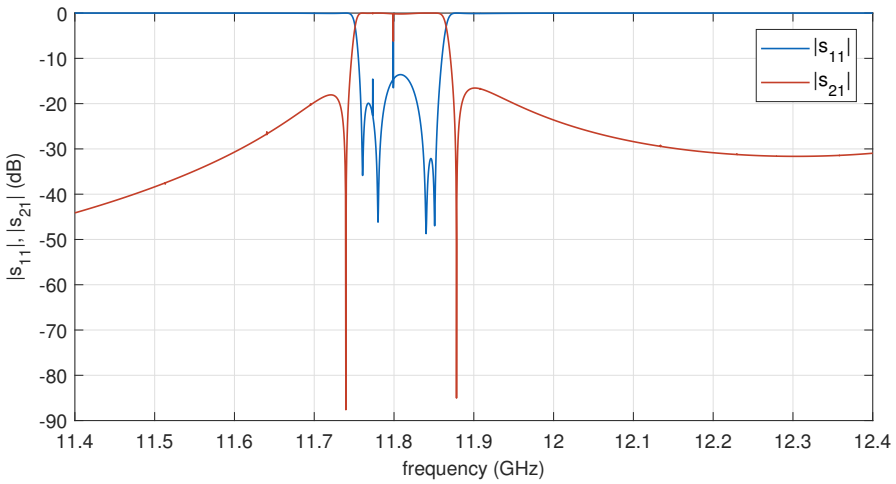


Figure 25: Scattering parameters computed with FEM-PMOR technique – the effect of spurious modes in band.

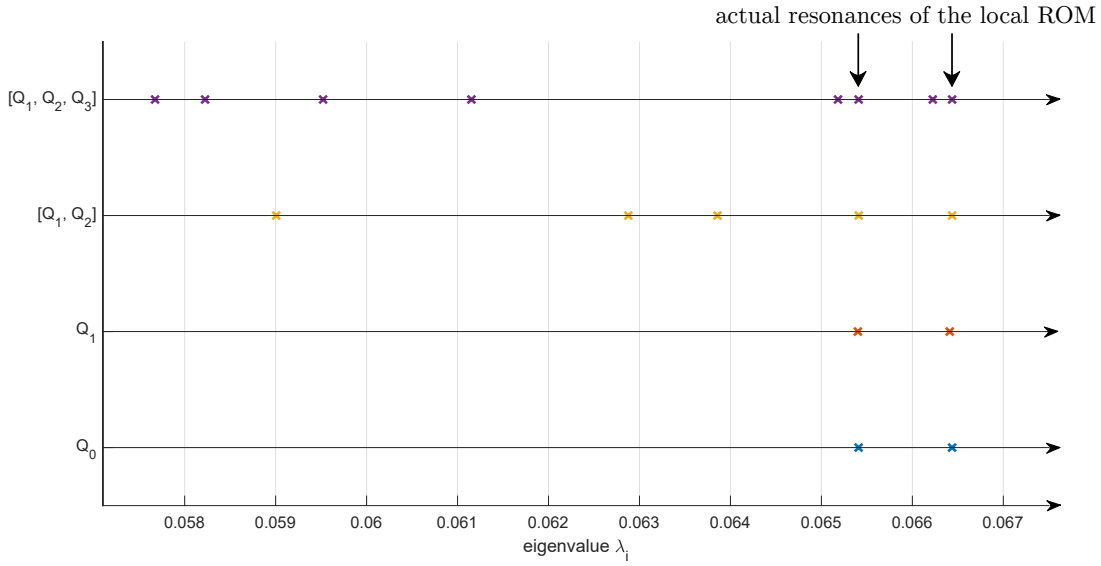


Figure 26: Eigenvalues of the local ROM in $\Omega_4$ obtained using accurate projection basis ($\mathbf{Q}_0$), single point parametrized projection basis ($\mathbf{Q}_1$), 2-point parametrized projection basis [$\mathbf{Q}_1$, $\mathbf{Q}_2$] and 3-points parametrized projection basis [$\mathbf{Q}_1$, $\mathbf{Q}_2$, $\mathbf{Q}_3$].

Next, the residue defined in eq. (6) are computed. The residue associated with spurious resonances should be small, while residue of the actual resonance should be higher. Residues computed for all eigenvalues in band of analysis are shown in Fig. 29. From the Fig. 29 it is apparent, that there are six spurious resonances with residues below 1e-2 and those should be deflated. The same resonances are identified as spurious using another criterion - the residue defined in 4 - see Fig. 30.

However, we might also observe the residues of eigenvalues out of band. – Fig. 31 shows residues of all eigenvalues of the local ROM. Based on the residues for all eigenvalues, 27 resonances have been identified as spurious (all resonances with residues below the dashed line in Fig. 31). Scattering parameters computed for the deflated reduced-order model are presented in Fig. 32 – good agreement with accurate filter response is obtained. There is no spurious resonances in band. Computing resonances of the global model gave only 4 resonances in band.

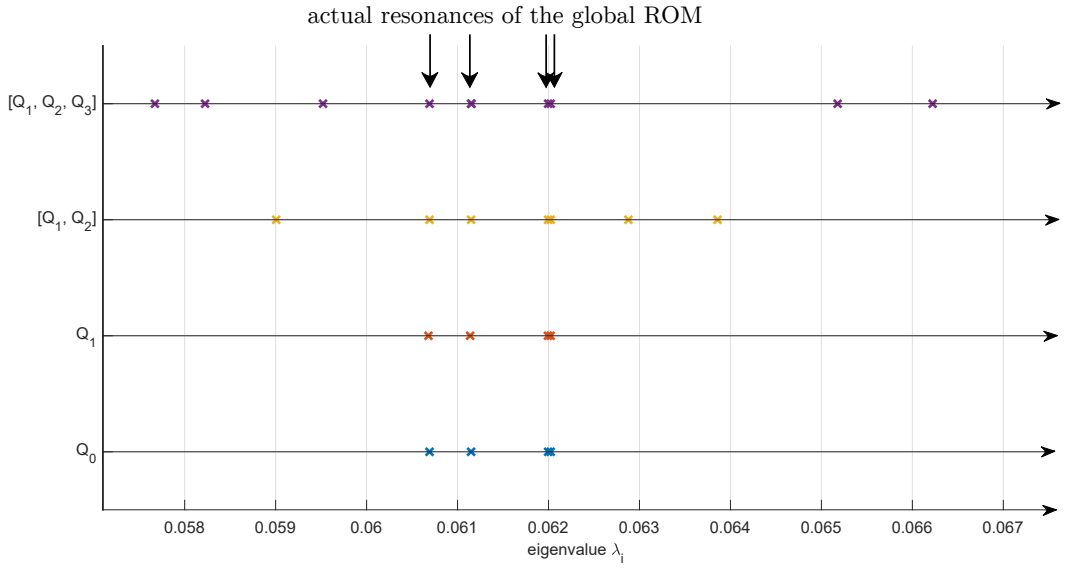


Figure 27: Eigenvalues of the global ROM - when using parametrized projection basis $[\mathbf{Q}_1,\ \mathbf{Q}_2]$ and $[\mathbf{Q}_1,\ \mathbf{Q}_2,\ \mathbf{Q}_3]$ spurious modes appear in the ROM.

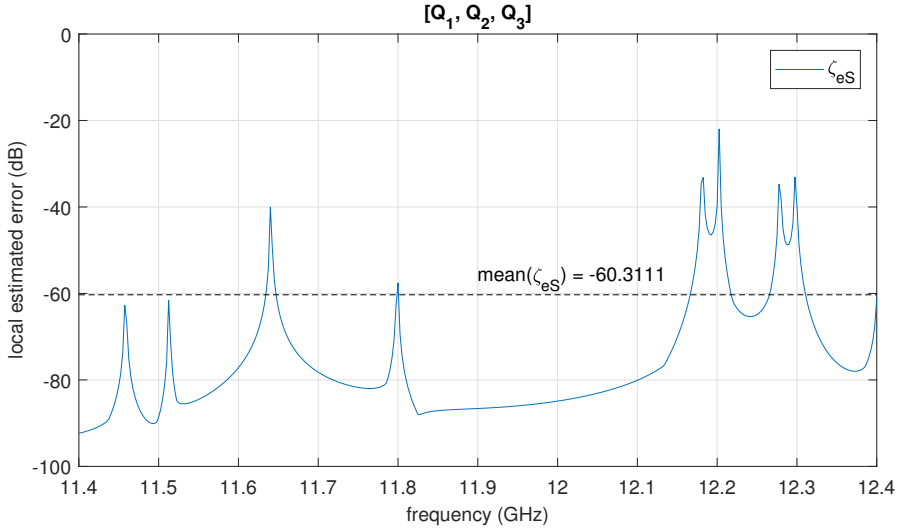


Figure 28: Local estimated error of the ROM in $\Omega_4$.

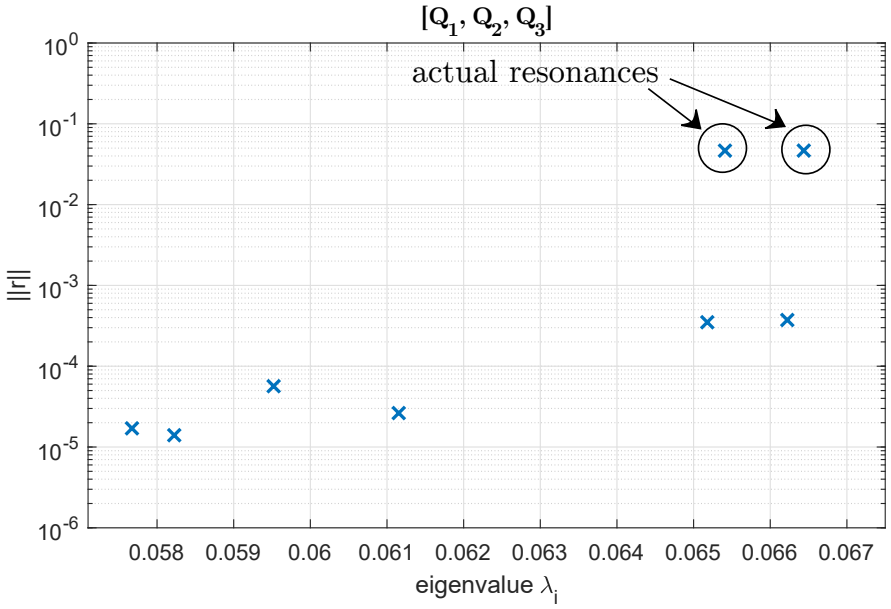


Figure 29: Residues (6) for eigenvalues of the ROM in frequency band of analysis.

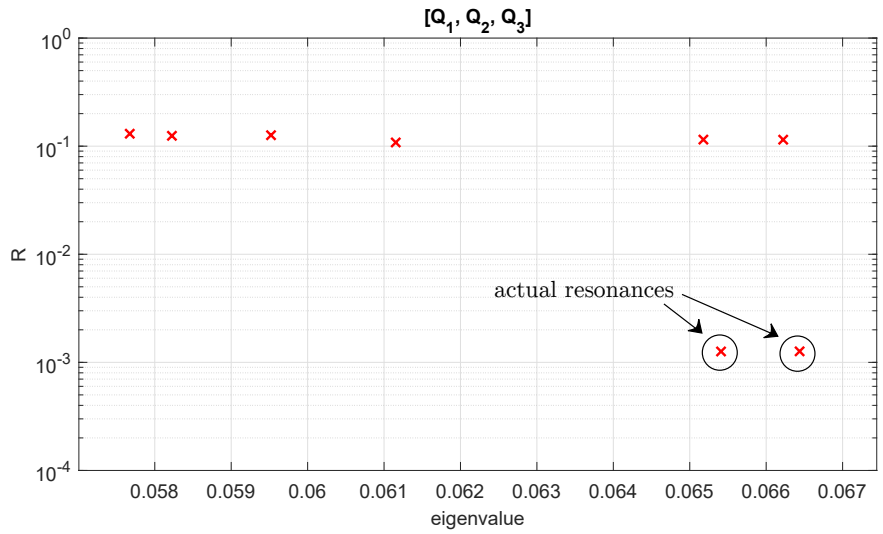


Figure 30: Residues (4) for eigenvalues of the ROM in frequency band of analysis.

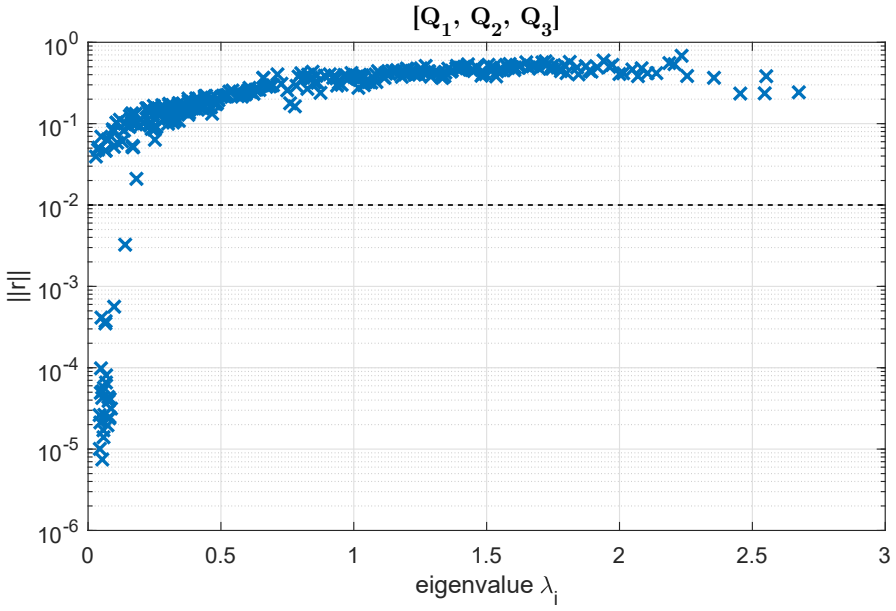


Figure 31: Residues for all eigenvalues of the ROM - 27 eigenvalues below the dotted line have been displaced (deflated) from the local ROM.

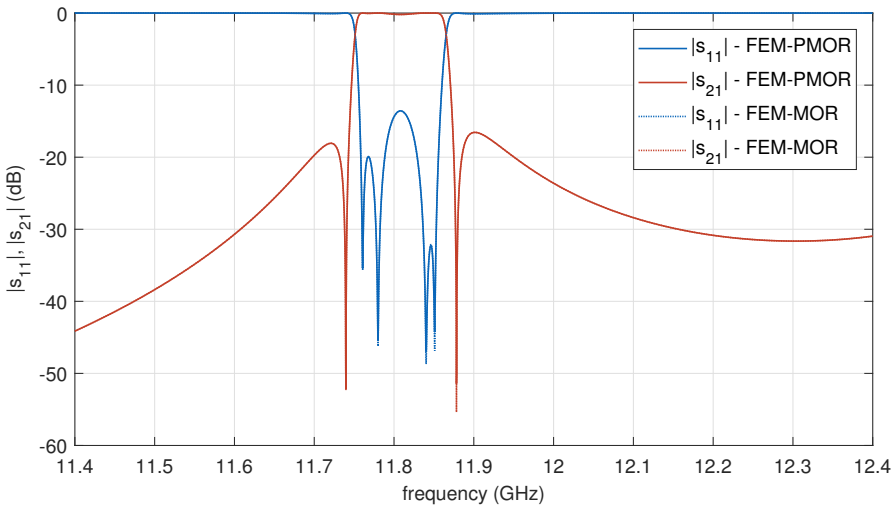


Figure 32: Scattering parameters obtained for deflated ROM – good agreement with accurate results and no spurious modes in frequency band of analysis.

## References

[1] G. Fotyga, K. Nyka, and M. Mrozowski, "Automatic Reduction Order Selection for Finite-Element Macromodels," 2017, submitted for publication.

[2] L. Hogben, *Handbook of linear algebra*. CRC Press, 2006.